

Isobaric Analog States in  $\text{Cl}^{35}$ 

D. D. WATSON, J. C. MANTHURUTHIL, AND F. D. LEE\*

Aerospace Research Laboratories, Wright-Patterson Air Force Base, Ohio†

(Received 26 June 1967)

The  $\gamma$ -ray yield from the  $\text{S}^{34}(p,\gamma)\text{Cl}^{35}$  reaction shows strong resonances at proton energies of 1214 and 1512 keV. These resonance states occur at the correct energies to be isobaric analogs of the 1.99- and 2.35-MeV states in  $\text{S}^{35}$ , respectively. Angular-distribution, triple-correlation, and polarization measurements have been performed at each of these resonances. The 1214-keV resonance, which corresponds to an excitation energy of 7.54 MeV in  $\text{Cl}^{35}$ , has spin and parity of  $\frac{7}{2}^-$ , and decays almost entirely to the 3.16-MeV level, which was also found to have spin and parity of  $\frac{7}{2}^-$ . The transition is pure M1 and has a measured strength of  $1.6 \pm 0.3$  Weisskopf units (W.u.). The 1512-keV resonance, which corresponds to an excitation energy of 7.84 MeV, has a spin and parity of  $\frac{3}{2}^-$ , and decays strongly to the 4.17-MeV level, which was found to be a  $\frac{3}{2}^-$  state. This transition is also pure M1 with a strength of  $1.0 \pm 0.3$  W.u. The value of  $\theta_p^2$  is about 0.2 for both the 1214-keV and the 1512-keV resonance, which compares favorably with the value of  $\theta_p^2 = \frac{1}{3}$  calculated for the pure single-nucleon  $f_{7/2}$ ,  $T = \frac{3}{2}$  and  $p_{3/2}$ ,  $T = \frac{3}{2}$  configurations respectively. This agrees with the large ( $d,p$ ) stripping width of the analog states at 1.99 and 2.35 MeV in  $\text{S}^{35}$ . The levels at 3.16 and 4.17 MeV appear to be of the same configuration as the corresponding resonance states, and to differ only in isobaric spin, having  $T = \frac{3}{2}$ . Values for the reduced widths, energies, and isobaric-spin splitting of the  $T_>$  and  $T_<$  states, and for the M1 transition speeds assuming pure single-nucleon states, have been calculated and are in good agreement with observed values.

## 1. INTRODUCTION

THE  $\gamma$ -ray yield curve for the  $\text{S}^{34}(p,\gamma)\text{Cl}^{35}$  reaction shows several resonances which are ten to twenty times stronger than the average resonance strength. These resonances occur at proton bombardment energies of 1214, 1512, 1895, 1900, 2078, and 2910 keV. The resonance at 1214 keV has been investigated<sup>1</sup> and is the  $T = \frac{3}{2}$  isobaric analog state of the first excited state in  $\text{S}^{35}$ . The state in  $\text{Cl}^{35}$  corresponding to the 1214-keV resonance has an excitation energy of 7.54 MeV, a spin and parity of  $\frac{7}{2}^-$ , and a strong M1 decay to a lower lying  $\frac{7}{2}^-$  state ( $T = \frac{1}{2}$ ) at 3.16 MeV. The observed M1 transition strength is  $1.6 \pm 0.3$  Weisskopf units (W.u.) as compared to a theoretical value of 2.2 W.u. for a single-particle ( $\frac{7}{2}^-, \frac{3}{2}$ )  $\rightarrow$  ( $\frac{7}{2}^-, \frac{1}{2}$ ) transition. The reduced proton width is  $\theta_p^2 = 0.2$  as compared to the pure single particle  $f_{7/2}$ ,  $T = \frac{3}{2}$  proton reduced width of 0.33. This leads one to interpret the 7.54 MeV state as an  $f_{7/2}$  single-nucleon state and the transition as being of the type ( $f_{7/2}$ ,  $T = \frac{3}{2}$ )  $\rightarrow$  ( $f_{7/2}$ ,  $T = \frac{1}{2}$ ). Similar examples can be found in other nuclei such as the  $E_p = 2294$ -keV resonance<sup>2</sup> in  $\text{Mg}^{26}(p,\gamma)\text{Al}^{27}$ , the  $E_p = 2187$ -keV resonance<sup>3</sup> in  $\text{Si}^{30}(p,\gamma)\text{P}^{31}$ , and the  $E_p = 1887$ -keV resonance<sup>4</sup> in  $\text{S}^{36}(p,\gamma)\text{Cl}^{37}$ . The resonances are all characterized by large reduced proton widths and all have spin and parity of  $\frac{7}{2}^-$ . They appear to be isobaric analogs of the 3.76-MeV level in  $\text{Mg}^{27}$ , 3.14-MeV level in  $\text{Si}^{31}$ , and the ground state of  $\text{S}^{37}$ , respectively. In fact similar  $f_{7/2}$  states are found throughout the  $s$ - $d$  shell. The energies of all these states are in good agreement with calcula-

tions if one assumes them to be single-nucleon states and accounts for effective binding energies, isospin, and Coulomb energies.<sup>5</sup>

In this paper we discuss experimental methods for the investigation of the analog states, the experimental results from the resonance at 1512-keV in  $\text{S}^{34}(p,\gamma)\text{Cl}^{35}$ , and discuss the characteristics of the single-particle analog states.

The resonance at 1512 keV appears to be primarily of the  $2p_{3/2}$  configuration and thus provides an interesting comparison to the  $1f_{7/2}$  resonance at 1214 keV. In the decay of the 1512-keV resonance we see a strong M1 transition of the type ( $2p_{3/2}$ ,  $T = \frac{3}{2}$ )  $\rightarrow$  ( $2p_{3/2}$ ,  $T = \frac{1}{2}$ ) and the reduced width is  $\theta_p^2 = 0.2$ , as was the case for the  $1f_{7/2}$  state. The energies and isospin splitting of the states involved are also in good agreement with

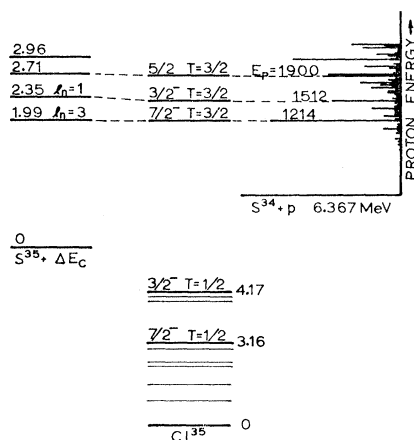


FIG. 1. Shown from left to right are the analog states in  $\text{S}^{35}$  corrected for the Coulomb displacement energy, the analog states in  $\text{Cl}^{35}$ , and the corresponding resonance yields in the  $\text{S}^{34}+p$  capture reaction. The states in  $\text{Cl}^{35}$  at 4.17 and 3.16 MeV are the  $T_<$  states corresponding to the  $\frac{3}{2}^-$  and  $\frac{7}{2}^-$   $T_>$  states.

\* N.R.C.-O.A.R.-Post Doctoral Associate.

† An element of the Office of Aerospace Research, U. S. Air Force.

<sup>1</sup> D. D. Watson, Phys. Letters **22**, 183 (1966).<sup>2</sup> D. M. Sheppard and C. Van der Leun, Nucl. Phys. **A100**, 333 (1967).<sup>3</sup> G. I. Harris, H. J. Hennecke, and F. W. Prosser, Jr., Phys. Letters **14**, 219 (1965).<sup>4</sup> A. K. Hyder and G. I. Harris, Phys. Letters **24B**, 273 (1967).<sup>5</sup> D. D. Watson and F. D. Lee, Phys. Letters **25B**, 472 (1967).

estimates based on an extreme single-particle description. A schematic indication of the  $\gamma$ -ray yield curve for  $S^{34}+p$  and the analog states is found in Fig. 1.

This work is part of a continuing investigation of the properties of the states in  $Cl^{35}$ .

## 2. TARGETS

Enriched targets of  $CdS$  (40%  $S^{34}$ ) deposited on tantalum backings were used for the early measurements of this experiment. These targets were found to be satisfactory for beam currents of approximately  $6 \mu A$ . During this work a method was developed for making  $Ag_2S$  targets from elemental sulfur enriched to 86% in  $S^{34}$ . A small quantity of sulfur is melted and the vapor allowed to pass over a silver target backing of thickness 10 mils which has been soldered to a  $\frac{1}{16}$ -in.-thick copper cooling disk.<sup>6</sup> Water cooled targets prepared in this manner have withstood beam currents as large as  $60 \mu A$  at 1.5 MeV with no appreciable deterioration. Such targets were used for the spectra and polarization measurements, in which the higher counting rates and improved background ratio were of particular importance.

## 3. $\gamma$ RAY YIELDS

Two large volume  $NaI(Tl)$  detectors placed at a distance of 2.5 cm from the target were used to locate the resonances and measure their widths. The coincidence counting rate between the two crystals was recorded for pulses corresponding to energies greater than 0.60 MeV. Therefore only  $\gamma$ -rays in cascade were counted. Since  $\gamma$  rays which arise from background or contaminant reactions such as  $F^{19}(p,\alpha\gamma)O^{16}$  and  $N^{15}(p,\alpha\gamma)C^{12}$  are predominantly one step transitions, this coincidence method resulted in greatly reduced off-resonance background. Shown in Fig. 2 are the coincidence yields at incident proton energies near 1200 and 1500 keV. In addition to the prominent 1214- and 1512-keV resonances, two small resonances are apparent

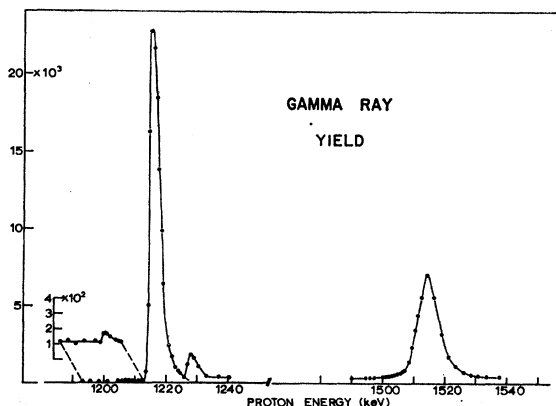


FIG. 2. The coincidence yield curve around the 1214- and 1512-keV resonances.

<sup>6</sup> D. D. Watson, Rev. Sci. Instr. 37, 1605 (1966).

at  $E_p=1207$  and  $1227$  keV. The former can only be seen on the expanded scale and is some 400 times smaller than the 1214-keV resonance.

The apparent width of the 1214-keV resonance from Fig. 2 is due entirely to beam resolution and target thickness, since the actual resonance width can be no more than 50 eV without having a reduced width in excess of the Wigner limit. The effect of the greater natural width of the 1512-keV resonance is evident in Fig. 2.

Since it is difficult to correct for angular-correlation effects in the coincidence yield, relative resonance strengths were determined from data obtained with a single biased detector placed at an angle of  $55^\circ$  with respect to the incident protons. These measurements have been corrected to give the total intensity of all primary  $\gamma$ -ray de-excitations. The measured total width of the 1512-keV resonance taken directly from the coincidence yield curve was 7.8 keV. The final value obtained for the resonance width by correcting for beam resolution and finite target thickness was  $5.0 \pm 0.5$  keV. The yield  $S = (2J+1)\Gamma_\gamma\Gamma_p/(\Gamma_\gamma+\Gamma_p)$  of this

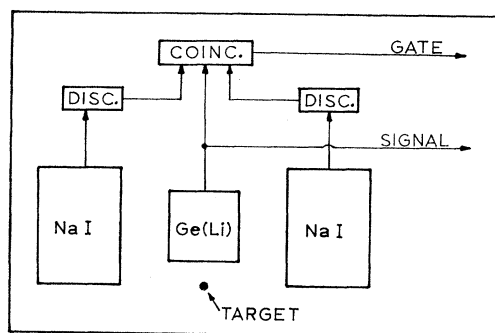


FIG. 3. A schematic diagram of the pair spectrometer.

resonance relative to that of the 1214-keV resonance was determined to be  $S_{1512} = 0.64 S_{1214}$ . Using the value  $S_{1214} = 21 \pm 3$  eV found by Engelbertnik and Endt,<sup>7</sup> we determine the absolute yield of the 1512 resonance to be  $13.5 \pm 2.4$  eV.

## 4. SPECTRA

Gamma-ray spectra were obtained with a  $20.3 \times 20.3$ -cm  $NaI(Tl)$  crystal and a  $12.7 \times 12.7$ -cm  $NaI(Tl)$  crystal. In order to determine accurate  $\gamma$ -ray energies and hence decay schemes, a 2-cc  $Ge(Li)$  solid state detector was used both in a conventional fashion and as the central element of a pair spectrometer as illustrated in Fig. 3. Direct spectra and pair-minus-two spectra obtained with the  $Ge(Li)$  detector at the 1214 and 1512-keV resonance appear in Figs. 4 and 5, respectively. The appearance of the 3.16-MeV  $\gamma$  ray in the decay of the 1512-keV resonance suggests the presence of weak

<sup>7</sup> G. A. Engelbertnik and P. M. Endt, Nucl. Phys. 88, 12 (1966).

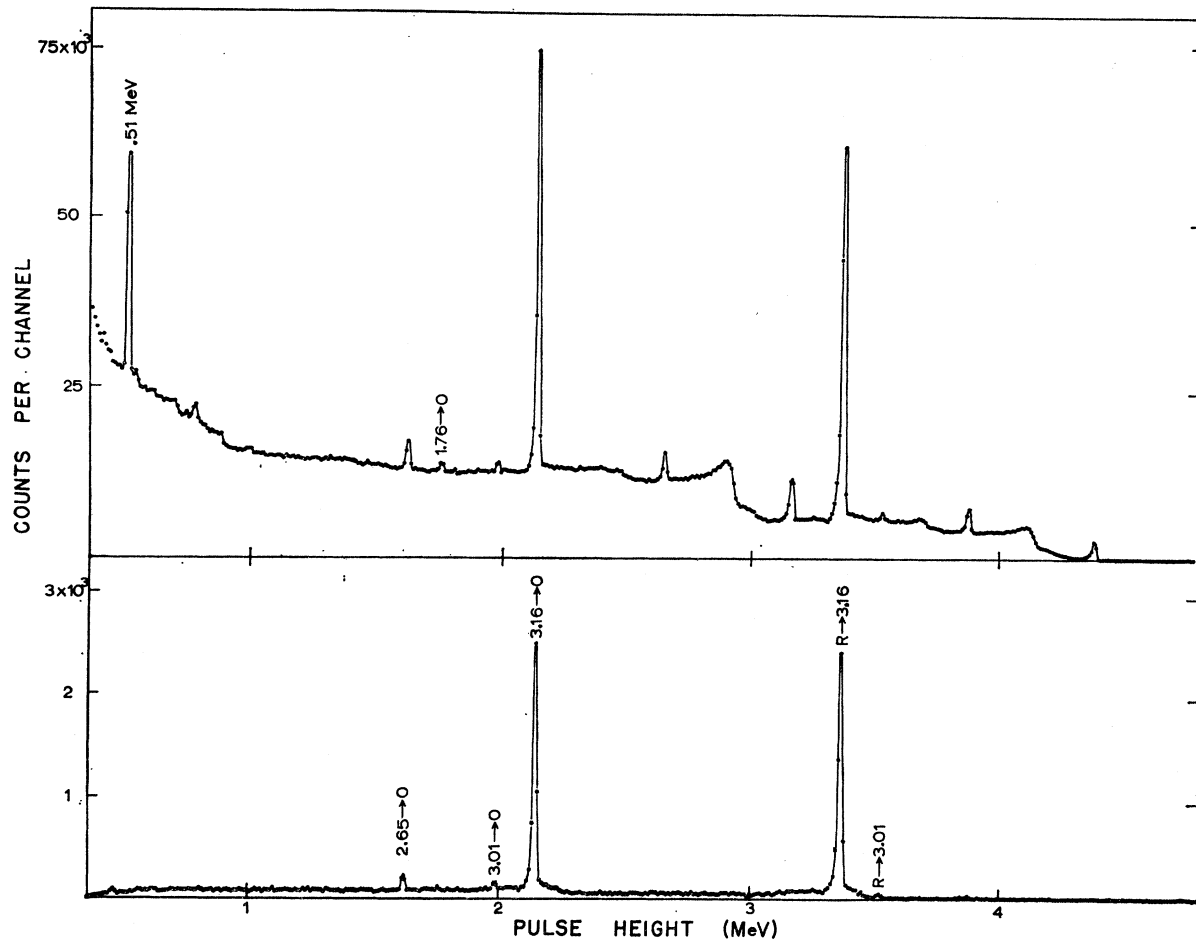


FIG. 4. Shown from top to bottom are the singles and the pair-minus-two spectra obtained with a 2 cc Ge(Li) detector at the 1214-keV resonance.

feeder  $\gamma$  rays to the 3.16-MeV level which are at present unaccounted for. The decay schemes for the two resonances are shown in Fig. 6. Relative  $\gamma$ -ray intensities and hence branching ratios were determined from the NaI spectra. All of the spectra obtained from the angular distribution and triple correlation measurements were first analyzed by a computer program which determines the relative intensities of the component  $\gamma$  rays by a least squares fit of standard  $\gamma$ -ray line shapes to the observed spectrum.<sup>8</sup> For each  $\gamma$  ray, the values of the intensity at the various angles were used in a second computer program to determine possible values of the spins of the levels involved, multipole mixing ratios for the radiation, and the function  $W = \sum A_{KM} X_{KM}(\theta_1, \theta_2, \phi)$  which best fits the data. The value of  $A_{00}$  is the correct intensity of the  $\gamma$  ray. The intensity terms obtained from the fits to the angular distribution and triple-correlation data are therefore average results obtained from 10 to 20

<sup>8</sup> H. D. Graber and D. D. Watson, Nucl. Instr. Methods 43, 355 (1966).

individual spectra. The triple-correlation spectra are particularly useful in determining branching ratios for the radiation from low-lying states which, in the singles spectra, are usually buried under background and Compton tails from higher-energy  $\gamma$  rays.

### 5. ANGULAR CORRELATIONS

For this experiment, the angular-correlation measurements were performed in two stages. Initially a detailed angular-distribution measurement was made and preliminary triple-correlation data taken. The results of these measurements were analyzed with the aid of the computer program previously mentioned in order to determine those spins and mixing ratios which minimize the function  $Q^2 = (1/N) \sum \omega_i [W(\Omega_i) - W^*(\Omega_i)]^2$ . In this case  $N$  is the number of degrees of freedom,  $\omega_i$  is a statistical weighting factor,  $W(\Omega_i)$  is the experimental counting rate at the  $i$ th set of detector angles  $\Omega_i$ , and  $W^*(\Omega_i)$  is the theoretical counting rate at  $\Omega_i$ .  $W^*(\Omega_i)$  is a function of the assumed spins and multipole mixing ratios. Since the ground state of  $\text{S}^{34}$  is a  $J=0$  state, the

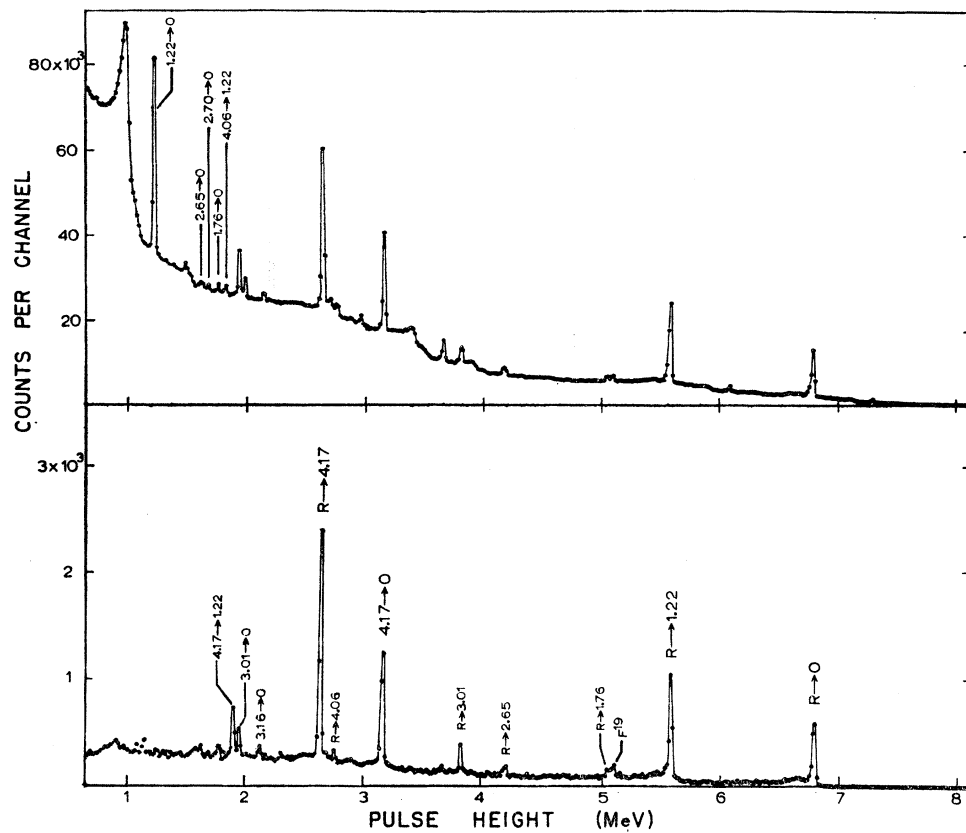


FIG. 5. Shown from top to bottom are the singles and the pair-minus-two spectra obtained with a 2 cc Ge(Li) detector at the 1512-keV resonance.

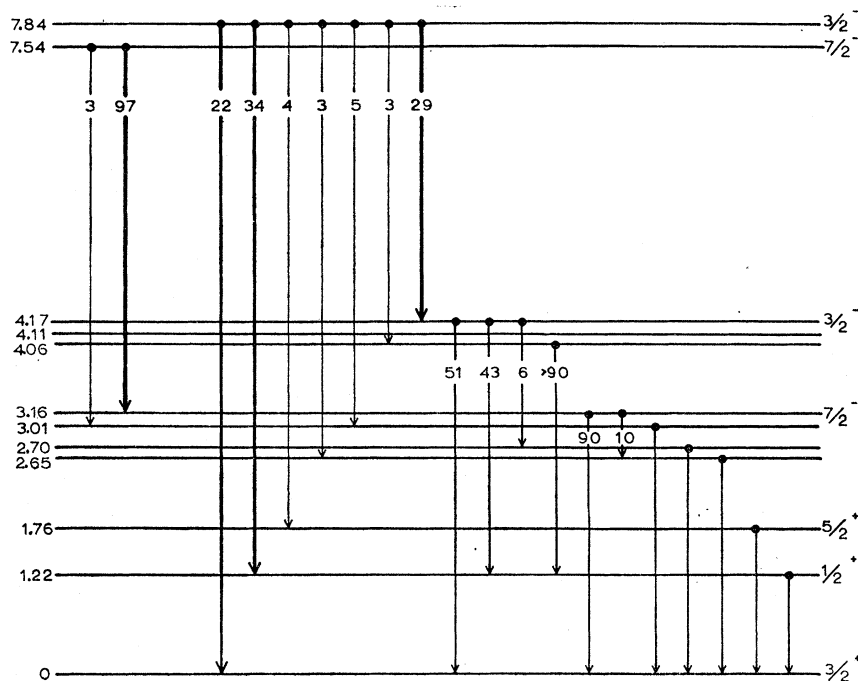


FIG. 6. The decay schemes and the branching ratios obtained from the de-excitation of the 7.54 and 7.84 MeV levels which correspond to the 1214- and 1512-keV resonances, respectively.

channel spin is uniquely  $\frac{1}{2}$  and therefore no formation parameters are involved in the analysis of the data. In terms of population parameter analysis which was used for this data, only the magnetic substates  $m = \pm \frac{1}{2}$  can be populated. In addition, symmetry requires that  $P_{1/2} = P_{-1/2} = 0.5$  and therefore the angular correlation can be written

$$W^*(\Omega_i) \propto \sum \frac{\delta_1^{p_1}}{1 + \delta_1^2} E_{KM}^N(J_1 L_1 L_1' J_{2, \frac{1}{2}}) \frac{\delta_2^{p_2}}{1 + \delta_2^2} \times h_M(J_2 L_2 L_2' J_3) X_{KM}^N(\Omega_i)$$

without specific reference to formation. The coefficients  $E_{KM}^N(J_1 L_1 L_1' J_{2, \frac{1}{2}})$  and  $h_M(J_2 L_2 L_2' J_3)$  are functions of the spins  $J_1$ ,  $J_2$ , and  $J_3$  of the states involved and of the multipolarity  $L_1 L_1'$ ,  $L_2$  and  $L_2'$  of the emitted radiations. These coefficients, along with the angular functions  $X_{KM}^N(\Omega_i)$  have been discussed and tabulated elsewhere.<sup>9,10</sup> The multipole mixing parameters  $\delta_1$  and  $\delta_2$  are defined as the ratio of reduced matrix elements of the multipole orders present in the primary and secondary radiation. Specifically,  $\delta = \langle J' \| L' \| J \rangle / \langle J' \| L \| J \rangle$ .

As is generally the case, the results of the angular distribution and preliminary triple-correlation measurements did not yield unambiguous spin and multipole mixing assignments for all the levels involved in the decay of the resonance. For each possible spin assignment however, sharp limitations on the values of the mixing ratios were obtained. With this information it was possible to design additional angular-correlation measurements of optimum sensitivity which resulted in decisive spin and mixing assignments. The measuring of these optimum correlations comprised the second stage of the experimental measurements.

The resonance at  $E_p = 1512$  keV provides an example of the procedure described above. Angular-distribution measurements on the ground-state transition,  $R \rightarrow 0$ , and the transition to the first excited state,  $R \rightarrow 1.22$ , result in a unique spin assignment of  $J_R = \frac{3}{2}$  for the resonance state. This is illustrated in Fig. 7, where for each possible spin assignment the value of  $Q^2$  is plotted for values of the multipole mixing ratio  $\delta$  between  $-\infty$  and  $+\infty$ . In actual practice, the substitution  $x = \arctan \delta$  is employed and values of  $Q^2$  are calculated in  $2.5^\circ$  steps in  $x$ . Since the values of  $Q^2$  as previously defined obey a  $\chi^2$  distribution, such curves are often called  $\chi^2$  curves. In this case the mean value of the  $\chi^2$  distribution is 1 and hence acceptable solutions for  $J$  and  $\delta$  would be those for which  $Q^2$  was approximately one. The 0.1% line, drawn at  $Q^2 = Q_0^2$  for example, indicates there is a statistical probability of 0.001 that the correct solution will have a measured value of  $Q^2$  which is greater than or equal to  $Q_0^2$ .

For the state at 4.17 MeV, acceptable fits to the

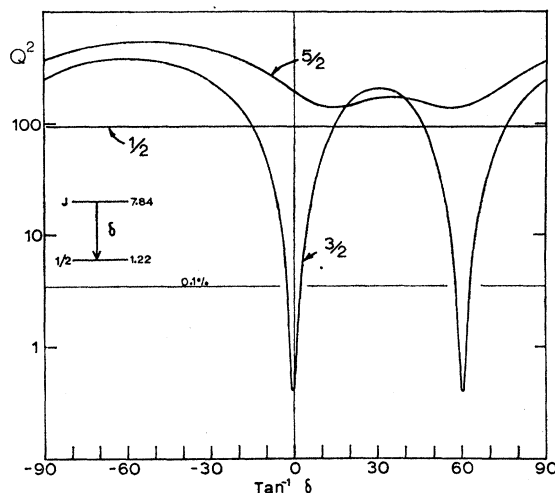


FIG. 7. The chi-squared plots obtained from the analysis of the angular distribution of the  $\gamma$  radiation from the Resonance  $\rightarrow 1.22$  level. Curves are shown for assumed resonance spins of  $J_{Res} = \frac{1}{2}$ ,  $\frac{3}{2}$ , and  $\frac{5}{2}$ .

angular distribution and preliminary triple-correlation data were obtained for spin assignments of  $J_{4.17} = \frac{1}{2}$ ,  $\frac{3}{2}$ , or  $\frac{5}{2}$ . For each possible choice of spin, a corresponding set of mixing ratios was uniquely determined. With this information it was possible to calculate the theoretical correlation, and hence the expected counting rate at many different angles, for each allowed set of spins and mixing ratios. Examination of the resulting theoretical correlations made clear a central problem in angular-correlation experiments as well as an obvious solution to the problem. In some angular configurations the predicted counting rates for the three possible choices of spin were quite different, but for many sets of angles the predictions were nearly identical, and data taken at these angles could be equally well fit by any choice of spin. It is clear that rather than pick an arbitrary set of angles for the correlation measurements, some of which would most probably be angles at which the correlations were nearly identical, one should concentrate his efforts on those angles where the correlations are quite distinct. In the case of the 4.17-MeV state, the following six sets of angles were chosen:  $(\theta_1, \theta_2, \phi)$  equals  $(90^\circ, V, 90^\circ)$  and  $(120^\circ, V, 180^\circ)$  where  $V$  takes on the values  $0^\circ$ ,  $45^\circ$ , and  $90^\circ$ . It was also clear from the calculated correlations that maintaining the relative normalization between the two geometries was of significant importance. Figure 8 shows the data obtained specifically to distinguish between an assignment of  $J_{4.17} = \frac{3}{2}$  and  $\frac{5}{2}$ . The solid and dashed lines are the theoretical best fits to the data points, each of which is the average of at least five independent measurements. The importance of maintaining the relative normalization between the two geometries is evident. A spin of  $J_{4.17} = \frac{5}{2}$  can be ruled out by inspection of Fig. 8 or by examining the minimum value of  $Q^2$  for

<sup>9</sup> D. D. Watson and G. I. Harris, Nucl. Data A3, 25 (1967).

<sup>10</sup> G. I. Harris, H. J. Hennecke, and D. D. Watson, Phys. Rev. 139, B1113 (1965).

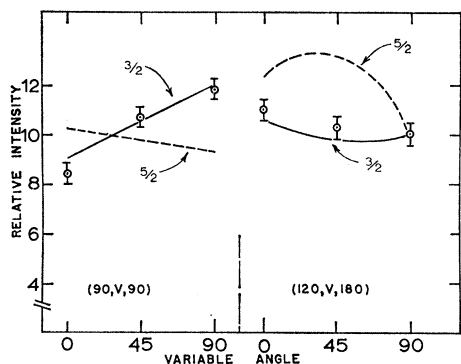


FIG. 8. The experimental data and the theoretical best fits obtained from the triple correlations designed to distinguish between the possible assignments of  $J=\frac{5}{2}$  or  $J=\frac{3}{2}$  for the 4.17-MeV level.

this assignment, as illustrated in Fig. 9. Similar evidence obtained from the  $R \rightarrow 4.17 \rightarrow 0$  cascade conclusively eliminates the  $J=\frac{1}{2}$  assignment. Hence the spin of the 4.17-MeV level is  $\frac{3}{2}$ . In order to reduce the error in the determination of the mixing ratios, a final analysis was made in which all of the angular-distribution and triple-correlation data was fitted simultaneously. At this point there were approximately 30 degrees of freedom for the statistical analysis. These results are summarized in Table I, along with the results obtained at the  $E_p = 1214$ -keV resonance which have been previously reported.<sup>1</sup> The spin ( $\frac{3}{2}$ ) of the 1512-keV resonance limits the complexity of the angular correlations to no more than terms in  $P_2(\cos\theta)$ . This condition results in two solutions for the mixing ratios. In most cases one of these solutions corresponds to an unreasonable transition speed and can be ignored. These cases are indicated in the table of results.

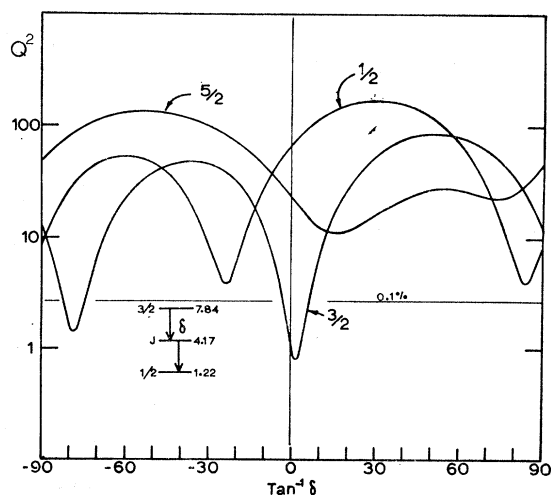


FIG. 9. The  $\chi^2$  plots obtained from the analysis of the data shown in Fig. 8.

## 6. POLARIZATION MEASUREMENTS

A Compton polarimeter was used to measure the linear polarizations of the  $\gamma$  rays from the 1214- and 1512-keV resonances in order to establish the parities of the levels discussed above. The polarimeter consisted of a  $5 \times 5$ -cm NaI scattering crystal oriented at  $90^\circ$  with respect to the axis of the incident proton beam and a pair of  $12.7 \times 12.7$ -cm NaI absorbing crystals, one mounted at  $0^\circ$  with respect to the reaction plane and the other mounted at  $90^\circ$  with respect to the reaction plane. The scattering and absorbing crystals were set for equal gains and the coincident pulses were electronically summed and stored in a multichannel analyzer. The electronic summing is used so that when a  $\gamma$  ray is Compton scattered from the scattering crystal and absorbed by one of the other crystals, the sum of the two pulses will be proportional to the full  $\gamma$ -ray energy. Thus the summed pulse height is independent of the scattering angle.

If  $N_0$  and  $N_{90}$  are the coincident counting rates measured at the  $0^\circ$  and  $90^\circ$  angles, then we can write

$$\frac{(N_{90} - N_0)/(N_{90} + N_0)}{= Q(W(90,90) - W(90,0))/(W(90,90) + W(90,0)) = QP,$$

where  $W(\theta, \phi)$  is the number of reaction  $\gamma$  rays per unit time emitted at an angle  $\theta$  with respect to the proton beam direction and having their electric vector at an angle  $\phi$  with respect to the reaction plane.  $W(\theta, \phi)$  depends upon the relative parity of the states emitting the radiation. The factor  $Q$  accounts for the polarization sensitivity of the Compton scattering process and also takes into consideration the finite detector size (geometry) of the polarimeter. This factor depends strongly on the energy of the incident  $\gamma$  radiation. The calculation of the polarization correlation function  $W(\theta, \phi)$  and the polarization sensitivity of the Compton polarimeter have been discussed by others.<sup>11-13</sup> A detailed account of the polarimeter we are using, including the calcula-

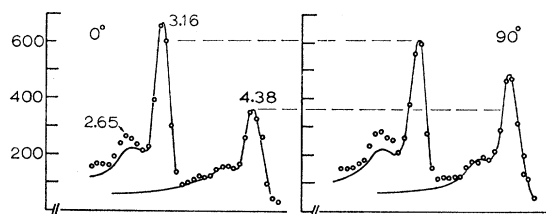


FIG. 10. An example of the data obtained at the 1214-keV resonance with the Compton polarimeter. The asymmetry in the scattered radiation is evident.

<sup>11</sup> L. W. Fagg and S. S. Hanna, Rev. Mod. Phys. **31**, 711 (1959).

<sup>12</sup> H. E. Gove and L. E. Litherland, in *Nuclear Spectroscopy*, edited by F. Azenberg-Selove (Academic Press Inc., New York, 1960), Part A.

<sup>13</sup> M. Suffert, P. M. Endt, and A. M. Hoogenboom, Physica **25**, 659 (1959).

TABLE I. A summary of results from the angular-correlation measurements. The transition speeds are given in Weisskopf units. The values in parentheses are allowed by the angular-correlation measurements but generally correspond to unreasonable transition speeds.

| Transition              | Branching ratio | Multipole mixing ratio                   | $ M ^2(L)$   | $ M ^2(L+1)$                     |
|-------------------------|-----------------|--|--|----------------------------------|
| 7.84 $\rightarrow$ 0    | 0.22            | $-0.02 \pm 0.03$<br>(3.6 $\pm 0.26$ )    | $E1 = 2.1 \times 10^{-3}$<br>( $E1 = 1.4 \times 10^{-4}$ ) | $M2 = 0.1 \pm 0.1$<br>$M2 = 140$ |
| 7.84 $\rightarrow$ 1.22 | 0.34            | $-0.06 \pm 0.03$<br>(3.1 $\pm 0.3$ )     | $E1 = 5.5 \times 10^{-3}$<br>( $E1 = 5.5 \times 10^{-4}$ ) | $M2 = 1 \pm 0.5$<br>$M2 = 520$   |
| 7.84 $\rightarrow$ 4.17 | 0.29            | $0.05 \pm 0.03$                          | $M1 = 1.0$   | $E2 = 0.7 \pm 0.6$               |
| 4.17 $\rightarrow$ 0    | 0.51            | $-0.06 \pm 0.03$<br>( $-3.08 \pm 0.30$ ) | ...  | ...                              |
| 4.17 $\rightarrow$ 1.22 | 0.43            | $-0.11 \pm 0.04$<br>(2.27 $\pm 0.30$ )   | ...  | ...                              |
| 7.54 $\rightarrow$ 3.16 | 0.97            | $0.07 \pm 0.02$                          | $M1 = 1.6$   | $E2 = 1.4 \pm 0.5$               |
| 3.16 $\rightarrow$ 0    | 0.90            | $-0.16 \pm 0.01$                         | ...  | ...                              |

tion of its sensitivity and finite geometry corrections will be given in a separate paper.<sup>14</sup>

The results of the polarization measurements are listed in Table II. The results of the measurements from the 1214-keV resonance indicate the sequence  $\frac{7}{2}^- \rightarrow M1 \rightarrow \frac{7}{2}^- \rightarrow M2 \rightarrow \frac{3}{2}^+$ . A spectrum obtained from the polarimeter at the 1214-keV resonance is shown in Fig. 10. The asymmetries between 0° and 90° are clearly visible and the sign of the asymmetry alone is enough to establish the parities. The polarization data from the 1512-keV resonance establishes the M1 character of the 7.84  $\rightarrow$  4.17 transition and indicates the 7.84  $\rightarrow$  0 ( $\frac{3}{2} \rightarrow \frac{3}{2}^+$ ) and 7.84  $\rightarrow$  1.22 ( $\frac{3}{2} \rightarrow \frac{1}{2}^+$ ) are E1 transitions. This results in negative parity assignments for the levels at 7.84 and 4.17 MeV. Inspection of Table II indicates that the parity of the 1512-keV resonance is not as conclusively established as the relative parity of the 7.84  $\rightarrow$  4.17 transition. However a positive parity assignment for this resonance would require d-wave proton capture which would imply a reduced proton width in excess of the Wigner limit. Hence, we conclude that the parity must be negative.

7. DISCUSSION

As mentioned previously, the resonance levels in  $Cl^{35}$  at 7.54 and 7.84 MeV ( $\frac{7}{2}^-$  and  $\frac{3}{2}^-$ , respectively) have the correct properties to be the isobaric analogs of the levels of  $S^{35}$  at 1.99 and 2.35 MeV ( $l_n=3$  and  $l_n=1$ , respectively). Furthermore, the properties of the  $\frac{7}{2}^-$

and  $\frac{3}{2}^-$  states in either nucleus can be predicted rather well by assuming that they are pure  $f_{7/2}$  and  $p_{3/2}$  single-nucleon configurations. A very simple model is useful for the formal discussion of the ideas expressed above. For the  $T = \frac{3}{2} (T_>)$  wave function of  $Cl^{35}$  we use the Clebsch-Gordan expansion of a  $T = 1, A = 34$  core, coupled to an extra-core nucleon. Explicitly

$$|TT_>\rangle = \sum C_{T_0 t_z T_z} T_0 t T |T_0 T_0 z\rangle |t t_z\rangle, \tag{1}$$

where

- $T$  = the isospin of  $Cl^{35}$ ,
- $T_0$  = the isospin of the core,
- $t$  = the isospin of the extra-core nucleon,

$C_{T_0 t_z T_z} T_0 t T$  is an isospin Clebsch-Gordan coefficient.

Hence

$$|Cl^{35} \frac{3}{2} \frac{1}{2}\rangle = (\frac{1}{3})^{1/2} |S^{34} + p\rangle + (\frac{2}{3})^{1/2} |Cl^{34} + n\rangle. \tag{2}$$

Similarly for the  $T = \frac{1}{2} (T_<)$  state

$$|Cl^{35} \frac{1}{2} \frac{1}{2}\rangle = (\frac{2}{3})^{1/2} |S^{34} + p\rangle - (\frac{1}{3})^{1/2} |Cl^{34} + n\rangle. \tag{3}$$

Thus we have two orthogonal single-nucleon states, one with  $T = \frac{3}{2}$  and the other with  $T = \frac{1}{2}$ . These two states are expected to differ in energy because of an assumed  $\beta t \cdot T_0$  interaction. The resonance states at 7.54 and 7.84 MeV are taken to be the  $T = \frac{3}{2}$  or  $T_>$  states and should therefore exhibit a proton width which is one-third of the total single-particle limit. Hence we would

TABLE II. A summary of results from the polarization measurements. The relative parity assignments are made by comparing the experimental polarization in column 3 with the theoretical values listed in columns 4 and 5.

| Transition              | Experimental asymmetry | Experimental polarization | Theoretical polarization |                  | Conclusion<br>Lowest-order multipole present |
|-------------------------|------------------------|---------------------------|--------------------------|------------------|--|
|                         |                        |                           | Parity change            | No parity change |  |
| 7.54 $\rightarrow$ 3.16 | 0.14 $\pm 0.02$        | +0.93 $\pm 0.1$           | -0.92                    | +0.92            | M1   |
| 3.16 $\rightarrow$ 0    | -0.12 $\pm 0.03$       | -0.75 $\pm 0.2$           | -0.71                    | +0.71            | M2   |
| 7.84 $\rightarrow$ 0    | -0.091 $\pm 0.06$      | -1.1 $\pm 0.8$            | -0.74                    | +0.74            | E1   |
| 7.84 $\rightarrow$ 1.22 | 0.015 $\pm 0.04$       | +0.17 $\pm 0.45$          | +0.60                    | -0.60            | (E1) <sup>a</sup>                            |
| 7.84 $\rightarrow$ 4.17 | 0.093 $\pm 0.026$      | +0.66 $\pm 0.18$          | -0.75                    | +0.75            | M1   |
| 4.17 $\rightarrow$ 0    | 0.015 $\pm 0.004$      | +0.12 $\pm 0.31$          | -0.73                    | +0.73            | (E1) <sup>a</sup>                            |

<sup>a</sup> See Text.

<sup>14</sup> F. D. Lee and D. D. Watson (to be published).

predict a reduced proton width for these states of 0.33 in units of  $\hbar^2/\mu a^2$  or an actual proton width of  $\Gamma_p = \frac{1}{3}P_l\hbar^2/\mu a^2$  where  $P_l$  is the Coulomb penetrability factor. The observed values of the reduced proton widths are both  $0.2 \pm 0.1$ . The major uncertainty in this number is due to the calculation of the penetrability. This is an extremely large reduced width and is in relatively good agreement with the single-particle prediction.

In order to compare the absolute binding energies of the states in  $\text{Cl}^{35}$  which are analogs of the states in  $\text{S}^{35}$ , we must correct for the Coulomb displacement energy  $\Delta E_c$  which arises when a neutron is replaced by a proton. An estimate of this Coulomb energy was made from the semi-empirical formula for odd  $A$  nuclei<sup>15</sup>

$$\Delta E_c = 1.44 \frac{\bar{Z}}{A^{1/3}} - 1.1 \text{ MeV},$$

where  $\bar{Z}$  is the average charge which in this case is equal to  $\frac{1}{2}(Z_{\text{S}^{35}} + Z_{\text{Cl}^{35}})$ . Ground-state binding energies were taken from the tables of Mattauch, Thiele, and Wapstra.<sup>16</sup>

The results of this calculation are

$\text{S}^{35}$  (1.99) corresponds to 7.53 MeV in  $\text{Cl}^{35}$ ,

$\text{S}^{35}$  (2.35) corresponds to 7.89 MeV in  $\text{Cl}^{35}$ ,

whereas the analog levels actually occur at 7.54 and 7.84 MeV. The energy difference between the  $f_{7/2}$  and  $p_{3/2}$  states in  $\text{S}^{35}$  is 0.36 MeV, while the energy difference between the analog states in  $\text{Cl}^{35}$  is 0.30 MeV. On the basis of our simple model for this system, the 60-keV difference in the  $f$ - $p$  splitting in  $\text{Cl}^{35}$  as compared to  $\text{S}^{35}$  may be attributed to a Coulomb energy difference of about 180 keV between  $f_{7/2}$  and  $p_{3/2}$  protons.

The  $T = \frac{1}{2}$  members of the single particle  $f_{7/2}$  and  $p_{3/2}$  excitations are split in energy far below the  $T = \frac{3}{2}$  members. This  $T_{>} - T_{<}$  splitting can be explained by assuming an interaction of the form  $\beta \mathbf{t} \cdot \mathbf{T}_0$  where  $\beta = V_1/A$  and  $V_1$  is independent of  $A$ .<sup>17</sup>

This term contributes an energy of

$$E_T = \frac{1}{2}\beta[T(T+1) - T_0(T_0+1) - t(t+1)]$$

to the single-nucleon states and results in a splitting given by

$$E_{T>} - E_{T<} = \frac{1}{2} \frac{V_1}{A} (2T_0 + 1).$$

A value of  $V_1(f_{7/2}) = 102$  MeV is required to explain the splitting between the  $\frac{7}{2}^-$ ,  $T = \frac{3}{2}$  level at 7.54 MeV and the  $\frac{7}{2}^-$ ,  $T = \frac{1}{2}$  level at 3.16 MeV. This is in good agreement with values for this parameter found by

<sup>15</sup> J. D. Anderson, C. Wong, and J. W. McClure, Phys. Rev. **138**, B615 (1965).

<sup>16</sup> J. H. E. Mattauch, W. Thiele, and A. H. Wapstra, Nucl. Phys. **67**, 1 (1965).

<sup>17</sup> A. M. Lane, Nucl. Phys. **35**, 676 (1962).

Sherr *et al.*,<sup>18</sup> Jaffe and Harchol,<sup>19</sup> and Hyder and Harris.<sup>4</sup> For the splitting between the  $\frac{3}{2}^-$ ,  $T = \frac{3}{2}$ ; and  $\frac{3}{2}^-$ ,  $T = \frac{1}{2}$  levels at 7.84 and 4.17 MeV one obtains  $V_1(p_{3/2}) = 86$  MeV.

If we assume that the wave functions of the  $T_{>}$  and  $T_{<}$  states discussed above are those appearing in Eqs. 2 and 3, then the  $M1$  transition speed between these states can be calculated. As provided by Talmi and Unna,<sup>20</sup>

$$\Gamma_\gamma(M1) = 2.76 \times 10^{-3} E_\gamma^3 \Lambda(M1) \text{ eV},$$

$$\Lambda(M1) = \frac{1}{2J+1} (f \|\Omega(M1)\| i)^2, \quad (4)$$

$$\Omega(M1) = \frac{1}{2}(g^p + g^n) \mathbf{j} + \frac{1}{2}(g^n - g^p) t_z \mathbf{j}.$$

The Schmidt values for the  $g$  factors are

$$g = -\frac{1}{j} (g_l l + \frac{1}{2} g_s) \quad \text{for } j = l + \frac{1}{2},$$

$$g = \frac{1}{j+1} [g_l(l+1) - \frac{1}{2} g_s] \quad \text{for } j = l - \frac{1}{2},$$

where  $g_l = 1$  for a proton,  $g_l = 0$  for a neutron,  $\frac{1}{2}g_s = 2.793$  for a proton, and  $\frac{1}{2}g_s = -1.913$  for a neutron. One may substitute the wave functions

$$|i\rangle = \frac{1}{(2T_0+1)^{1/2}} |11\frac{1}{2} - \frac{1}{2}\rangle + \frac{(2T_0)^{1/2}}{(2T_0+1)^{1/2}} |10\frac{1}{2} \frac{1}{2}\rangle$$

and

$$|f\rangle = \frac{(2T_0)^{1/2}}{(2T_0+1)^{1/2}} |11\frac{1}{2} - \frac{1}{2}\rangle - \frac{1}{(2T_0+1)^{1/2}} |10\frac{1}{2} \frac{1}{2}\rangle$$

into formula (4) to obtain

$$\Gamma_\gamma(M1) = 2.76 \times 10^{-3} E_\gamma^3 \frac{2T_0}{(2T_0+1)^2} J(J+1) (g^n - g^p)^2,$$

or in terms of Weisskopf units using  $\Gamma_W(M1) = 0.021 E_\gamma^3$  eV we have

$$|M|^2(M1) = 0.13J(J+1)(g^n - g^p)^2 2T_0 / (2T_0+1)^2 \text{ W.u.}$$

In the case under consideration  $T_0 = 1$ , which yields

$$|M|^2(M1) = 2.2 \text{ Wu} \quad \text{for the } 7.54 \rightarrow 3.16 \text{ transition,}$$

$$|M|^2(M1) = 1.6 \text{ Wu} \quad \text{for the } 7.84 \rightarrow 4.17 \text{ transition.}$$

The observed values of 1.6 and 1.0 Wu, respectively are in good agreement with the above single-particle transition speeds. These results are summarized in Table III.

The absence of any resonances of significant strength

<sup>18</sup> R. Sherr, B. F. Bayman, E. Rost, M. E. Rickey, and C. G. Hoot, Phys. Rev. **139**, B1272 (1965).

<sup>19</sup> A. A. Jaffe and M. Harchol, *Isospin in Nuclear Physics* (Academic Press Inc., New York, 1966), p. 835.

<sup>20</sup> I. Talmi and I. Unna, Ann. Rev. Nucl. Sci. **10**, 353 (1960).



TABLE III. A summary of results for the reduced widths and from the considerations of isobaric spin.

| Level | $J$           | $T$           | Reduced width                | Single-particle limit | Energy calculated from $\text{S}^{35}$ analog levels (MeV) | Resonance strength | $T$ splitting | $V_1$ (MeV) |
|-------|---------------|---------------|------------------------------|-----------------------|--|--------------------|---------------|-------------|
| 7.54  | $\frac{7}{2}$ | $\frac{3}{2}$ | $\theta_p^2 = 0.2 \pm 0.1^a$ | $\theta_p^2 = 0.33$   | 7.35   | $2.6 \pm 0.4$ eV   | 4.38 MeV      | 102         |
| 3.16  | $\frac{7}{2}$ | $\frac{1}{2}$ |                              |                       |  |                    |               |             |
| 7.84  | $\frac{3}{2}$ | $\frac{3}{2}$ | $\theta_p^2 = 0.2 \pm 0.1^a$ | $\theta_p^2 = 0.33$   | 7.89   | $3.4 \pm 0.6$ eV   | 3.67 MeV      | 86          |
| 4.17  | $\frac{3}{2}$ | $\frac{1}{2}$ |                              |                       |  |                    |               |             |

<sup>a</sup> Recent calculations of the reduced widths using a computer code from J. P. Schiffer of Argonne National Laboratory have resulted in the value  $0.20 \pm 0.02$  for the reduced width of the 7.84-MeV level. This result is based upon a nuclear radius of  $1.4 (A^{1/3} + 1)$  F. Because of the uncertainty in the experimental value of the proton width of the 7.54-MeV level, we were unable to obtain a more accurate value of its reduced width.

in the neighborhood of the 1214- and 1512-keV resonances together with the large reduced widths of these resonances indicates that the single-particle excitations are not mixing to any appreciable extent with nearby  $T = \frac{1}{2}$  states of the same spin and parity. Evidently at

this low excitation energy the  $T = \frac{1}{2}$  states are still widely spaced relative to the strength of the isospin breaking interactions, although at higher excitation energies there is some evidence for isospin mixing. Further investigation of these effects is now in progress.

## Energy Dependence of $(p, p' \gamma)$ Correlations in $\text{Ti}^{48}$ †

H. J. HAUSMAN, R. M. HUMES,\* AND R. G. SEYLER

*The Ohio State University, Columbus, Ohio*

(Received 27 July 1967)

Absolute double-differential cross sections have been measured at ten bombarding energies from 4–6 MeV for the reaction  $\text{Ti}^{48}(p, p' \gamma)0.99$  MeV. The angular correlations were measured with the  $\gamma$ -ray detector moving in a plane perpendicular to the reaction plane. Comparisons are made between the measured cross sections and the predictions of the statistical compound-nucleus theory. At all bombarding energies, angular correlations were measured at two supplementary (c.m.) proton-detector angles in order to check the symmetries predicted by statistical theory. Attempts are made to ascribe deviations of the experimental correlations from statistical-model predictions to the presence of direct reactions. The angular dependence of the spin-flip cross section was measured at three bombarding energies: 5.16, 5.25, and 5.46 MeV. In addition, the energy dependence of the spin-flip cross section was measured at a laboratory proton-detector angle of  $131^\circ$ . For that geometry wherein the proton detector is in the backward quadrant, agreement between the measured correlations and statistical-model predictions is very good.

### I. INTRODUCTION

IN recent years there has been considerable interest in the study of angular (triple) correlations between inelastically scattered nucleons and their associated de-excitation  $\gamma$  rays as a tool for studying reaction mechanisms. Many of these studies have been made at relatively high energies with consequent comparison to direct interaction (DI) theory. Sheldon<sup>1</sup> has shown, however, that in many of these cases, especially for atomic masses greater than 40, the results may be fitted reasonably well by statistical compound-nucleus (CN) correlation theory.

As a more sensitive test for the admixture of CN and

DI mechanisms, Sheldon<sup>1,2</sup> has suggested the study of noncoplanar radiations. In a previous paper<sup>3</sup> in which the angular dependence of the correlation function for  $\text{Ti}^{48}$  was studied at two energies, the authors noted an apparent symmetry breakdown which indicated that the normal-plane correlation function may provide a more sensitive measure of the CN-DI admixture than reaction-plane correlations. The present paper reports the extension of these normal-plane correlations to a series of ten bombarding energies corresponding to peaks and valleys in the excitation curve above and below the Coulomb barrier and the  $(p, n)$  threshold.

Model-independent symmetries associated with particle- $\gamma$ -ray angular correlations can, in certain circumstances, aid in the analysis of reaction mechanisms.

† This work was supported in part by the National Science Foundation under Grant No. GP-2210.

\* Present address: Pacific Northwest Laboratory, Richland, Washington.

<sup>1</sup> E. Sheldon, *Rev. Mod. Phys.* **35**, 795 (1963).

<sup>2</sup> E. Sheldon, *Phys. Letters* **2**, 178 (1962).

<sup>3</sup> R. M. Humes and H. J. Hausman, *Phys. Rev.* **139**, B846 (1965).